Cylinder Detection and Grasping Application Using Humanoid Robot

Shingo Maeda, Tomohito Takubo,
Kenji Inoue, Tatsuo Arai
Graduate School of Engineering Science
Osaka University
1-3 Machikaneyama, Toyonaka, Osaka, 560-8531, Japan
maeda@arai-lab.sys.es.osaka-u.ac.jp

Shun Nishide
Graduate School of Informatics
Kyoto University
Engineering Building #10, Sakyo, Kyoto, 606-8501,
Japan

Abstract: Researches on humanoid robots have become more and more active in various fields. One of the purposes is to construct a coexistent and cooperative society between humanoid robots and human. The body of humanoid robots is similar to human beings enabling them to walk with a pair of legs and to work with their hands. Therefore, humanoid robots have advantages to work in human environment. So, researchers' interests are attracted to introduce them into construction sites for more efficient works. In this paper, the main objective is the process of grasping experiment by a humanoid robot as an example of such application. The robot is required to obtain the object information and the grasping point. We propose a detection method for cylinders using L*a*b* color discrimination and oval estimation with conic fitting. The grabbing experiment using HRP-2 denotes the effectivity of the method using the GUI for transmitting commands.

Keywords: Grasping, Cylinder Detection, GUI, Humanoid Robot

1. INTRODUCTION

Decrease of the productive age has become a severe issue for the construction industry. So, robotic researchers have considered introduction of robots into construction works to compensate for insufficiency of workers. Examples of such works include menial works, human cooperative works, and deputies working at dangerous places. It is expected that efficiency, economy and safety in the construction site will be improved by change of main subject of works from human beings to robots [1].

Researches on humanoid robots have become more and more active in various fields. One of the purposes is to construct a coexistent and cooperative society between humanoid robots and human. The body of humanoid robots is similar to human beings enabling them to walk with a pair of legs and to work with their hands [2-3]. Humanoid robots have advantages to work in human environment. Researchers' interests are attracted to introduce them into construction sites for more efficient works [4-6]. In construction sites, many object consist simple shapes, such as pipes or blocks. We consider humanoid robots can substitute for human beings in the work dealing with these objects.

In this paper, we assume a case where the target object is a cylinder, which is easy to grab, and describe the process of object grabbing experiment. In chapter 2, we illustrate the method of recognition of cylinder with color detection and estimation of cylindrical shape. In chapter 3, we implement the control system to the humanoid robot and evaluate the system using GUI.

2. RECOGNITION OF OBJECT POSITION

2.1 Color Discrimination with L* a* b* Color Expression

In this research, MiniBEE, developed by View PLUS CO., Ltd. is used as a stereo vision system to recognize the 3-D environmental information. It is set into the head of the humanoid robot HRP-2 developed by Kawada Industries, INC. The state of head is shown in Fig. 1.

MiniBEE can obtain position (x_n, y_n, z_n) and color (R_n, G_n, B_n) information of data points in the visible area.

In order to acquire accurate stereo correspondence, we use a cylinder with random marked lines. When a point on the cylinder is clicked, all of the pixels with similar color elements around the clicked point are extracted. These pixels can be transformed into 3-D data by the stereo processing library in Mini BEE.

However, the brightness of the cylinder differs from place to place due to the reflection of light. Therefore, when we

Fig.1 Stereo Camera MiniBEE in the Head of HRP-2

use (R_n, G_n, B_n) color values, the detection is difficult because these values are affected easily by light condition. To detect the cylinder, a detection method which is robust over the light condition is necessary.

Then, we transformed (R_n, G_n, B_n) to (L^*_n, a^*_n, b^*_n), where L^*, a^*, and b^* each indicate brightness, hue, and saturation. The transform equation can be expressed as follows;

$$\begin{bmatrix} X \\ Y \\ Z \end{bmatrix} = \begin{bmatrix} 0.61 & 0.17 & 0.20 \\ 0.30 & 0.59 & 0.11 \\ 0.00 & 0.07 & 1.12 \end{bmatrix} \begin{bmatrix} R \\ G \\ B \end{bmatrix} \quad (1)$$

$$\begin{aligned} L^* &= 116 f(Y/Y_n) - 16 \\ a^* &= 500\{f(X/X_n) - f(Y/Y_n)\} \\ b^* &= 200\{f(Y/Y_n) - f(Z/Z_n)\} \end{aligned} \quad (2)$$

$$\begin{aligned} &Case: X/X_n > 0.008856 \\ &f(X/X_n) = (X/X_n)^{1/3} \\ &Case: X/X_n \le 0.008856 \\ &f(X/X_n) = 7.787(X/X_n) + 16/116 \end{aligned} \quad (3)$$

The values (X_n, Y_n, Z_n) indicate the values (X, Y, Z) of room light [7]. In this method, each pixel possesses individual values of (L^*_n, a^*_n, b^*_n), and we can ignore the value of L_n^* to remove the effect of light condition. Now, the values of (a*, b*) of the clicked point is defined as (A, B), when both $|A - a_n^*|$ and $|B - b_n^*|$ are less than threshold value (we define the value 15 in the experiment), the pixel is extracted. By repeating this process, all of the colored pixels of the cylinder are extracted. The result of extraction is shown in Fig. 2. We can see that this color detecting process can extract all of visible area on the clicked cylinder.

2.2 Detection of Center of Gravity by Conic Fitting

The detected 3D cylindrical data points are shown in Fig.3. In this data, there is only upper half part of the cylinder. For stable manipulation, the humanoid robot should grasp the center of gravity of the cylinder. However, it cannot be calculated from only the upper half of the cylinder. To estimate the center of the gravity of the cylinder, we use "conic fitting" and cylindrical model.

Conic is the general term of a curve with second order such as oval (including the circle), parabola and hyperbola. There are a lot of artificial objects consisting of circle, sphere and et al, and its shape of section can be expressed by the conic. Therefore, conic fitting is used in various recognition systems [8].

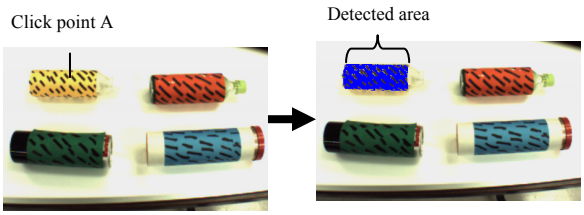

Fig. 2 Extraction around the clicked point

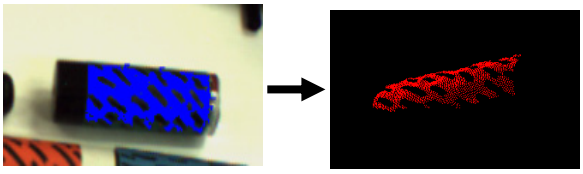

Fig. 3 Transform to 3D data

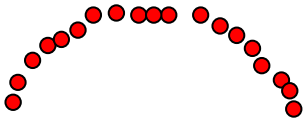

Fig. 4 Obtained points data

If we can get a part of oval shape from data points as shown in Fig.4, we can estimate the center of oval by conic fitting algorithm.

As preprocessing of conic fitting, we assume the value of the position vector $p_a = (x, y, z)$ to $x_a(0), x_a(1), x_a(2)$ and define the covariance matrix $V[x_a]$, noise level ε, so that the equation can be expressed as follow;

$$V[x_a] = \varepsilon^2 V_0[x_a] \quad (4)$$

Here, $V_0[x_a]$ denotes regularized covariance matrix.

The algorithm of conic fitting is shown as follows.

Input: Data points $\{p_a\}_{a=1}^N$ (N is the number of data points)

Output: Matrix Q

Algorithm:

step1. Set variables c = 0, $W_a = 1$, $a = 1, \cdots N$

step2. Calculate the tensor $\mathrm{M} = M_{ijkl}$ and $\mathrm{N} = N_{ijkl}$

$$M_{ijkl} = \frac{1}{N} \sum_{a=1}^{N} W_a x_a(i) x_a(j) x_a(k) x_a(l) \quad (5)$$

$$\begin{aligned} N_{ijkl} = \sum_{a=1}^{N} W_a \big(& V_0[x_a]_{ij} x_a(k) x_a(l) \\ & + V_0[x_a]_{ik} x_a(j) x_a(l) + V_0[x_a]_{il} x_a(j) x_a(k) \\ & + V_0[x_a]_{jk} x_a(i) x_a(l) + V_0[x_a]_{jl} x_a(i) x_a(k) \\ & + V_0[x_a]_{kl} x_a(i) x_a(j) \big) \end{aligned} \quad (6)$$

step3. Calculate the 6 eigenvalues of tensor $\hat{\mathrm{M}}$, $\lambda_1 \geq \cdots \geq \lambda_6$, and the corresponding orthonormal eigenmatrix $\{Q_1, \cdots, Q_6\}$.

$$\hat{\mathrm{M}} = \mathrm{M} - c\mathrm{N} \qquad (7)$$

step4. If $\lambda_6 \approx 0$ does not hold, renew the value c, W_a as follows.

$$c \leftarrow c + \frac{\lambda_6}{(Q_6, \mathrm{N}Q_6)}, W_a \leftarrow \frac{1}{4(x_a, Q_6 V_0[x_a]Q_6 x_a)} \qquad (8)$$

step5. Set the matrix Q_6 as Q and return Q.

The method is so robust that if there is large noise, the solution converges immediately[9].

Using this algorithm, the shape of the conic can be estimated from raw data points. However, the obtained data consists of only the upper half part of the oval, if the margin error of the raw is large, not only oval but also parabola and hyperbola can be fitted.

We can get Matrix Q as following shape.

$$Q = \begin{pmatrix} A & B & D/f \\ B & C & E/f \\ D/f & E/f & F/f^2 \end{pmatrix} \qquad (9)$$

The elements $(A, B, \cdots, F)$ are the coefficients of conic equation. It is shown as follows;

$$Ax^2 + 2Bxy + Cy^2 + 2(Dx + Ey) + F = 0 \qquad (10)$$

f is a scalar to transform the order of x/f and y/f to 1.

The way of decision whether this conic is oval or not is shown as follows;

If det Q > 0, multiply -1 to both sides and transform to det Q < 0.

- $AC - B^2 < 0$ The type of conic is hyperbola.
- $AC - B^2 = 0$ The type of conic is parabola.
- $AC - B^2 > 0$
  - $A + C > 0$ The type of conic is oval.
  - $A + C < 0$ Degenerate to a straight line, double straight line, a point or an empty set.

When the conic is estimated as a part of the oval, the center point of oval $P = (p, q)^T$ is calculated with parameters A, B, C, D, E as shown in follows;

$$P = \begin{pmatrix} p \\ q \end{pmatrix} = \begin{pmatrix} A & B \\ C & D \end{pmatrix}^{-1} \begin{pmatrix} -\frac{D}{f} \\ -\frac{E}{f} \end{pmatrix} \qquad (11)$$

The process of calculating the center of gravity of the cylinder using conic fitting is described as follows;

1. We calculate the tentative center of gravity and the principal axis of upper half pipe using the captured pixels' data (Fig. 5).
2. We divide the data of half pipe every 3mm by perpendicular plane along the principal axis from tentative center of gravity as shown in Fig.6. Thus, we get the row of data points like Fig. 4 in every space between adjacent planes.
3. If there are 5 or more data points between the adjacent planes, the conic fitting is done in the plane. If the conic is a part of oval, plot the center point of the oval.
4. The candidate of the center line is drawn by least squares method based on the center point of each oval. Furthermore, slide the perpendicular plane every 3mm along the candidate of the center line. If there are 5 or less data points between the adjacent perpendicular planes, delete the candidate of the center line. The remained part of the candidate is the center line of the whole cylinder. The length of the line is the length of the cylinder and the center point of the center line is assumed the center of gravity of the cylinder. The positions of center line and center point of the cylinder are shown in Fig. 7.

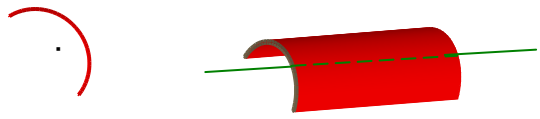

Fig.5 Tentative center of gravity and principal axis of half pipe

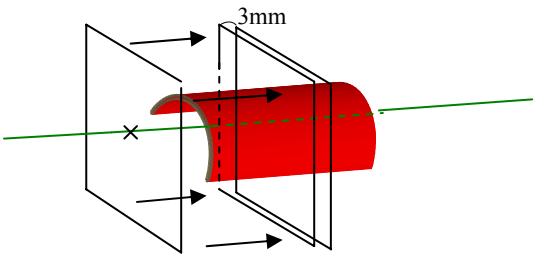

Fig. 6 Division of half pipe along principal axis

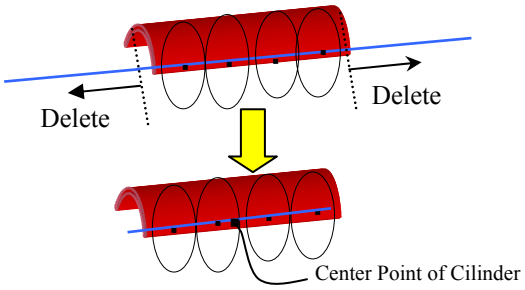

Fig. 7 Center line and center point of cylinder

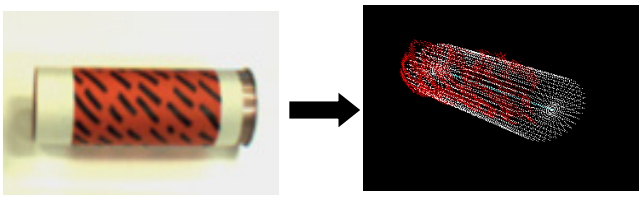

Fig. 8 Result of conic fitting

The calculated center line is fitted with the center line of the cylinder model. Thus, we can fit the cylinder model to the captured upper half data of the cylinder with conic fitting as shown in Fig.8. We call the center of gravity of the cylinder as "target point" from now.

3. GRSPING EXPERIMENT WITH THE HUMANOID ROBOT

We experiment grasping application with humanoid robot using cylinder detecting algorism. In this experiment, we controlled the humanoid robot HRP-2 with a GUI. The GUI display is based on the image captured by Mini BEE set on the head of HRP-2.

3.1 The Specification of GUI Control System

We develop GUI application for controlling HRP-2 and implement it on a tablet PC. The PC can be held with hand as shown in Fig. 9. Fig. 10 shows GUI image. HRP-2 can receive commands by socket connection. The controller can command HRP-2 by clicking the objects or icons on the image. The functions are described in the following paragraph.

A. Click point:

When an object in the image is clicked, the similar color elements are extracted in the vicinity of the selected pixel using the color detection method of section 2.1. The position (x, y, z) of clicked point is also calculated using the stereo processing library in Mini BEE.

B. Neck turning button:

When the object is out of camera, the user can turn the neck to put the object into sight. When the turning button is pushed, HRP-2 turns the neck according to the Scroll bar. Furthermore, HRP-2 can turn the neck to its initial position when the reset button is pushed.

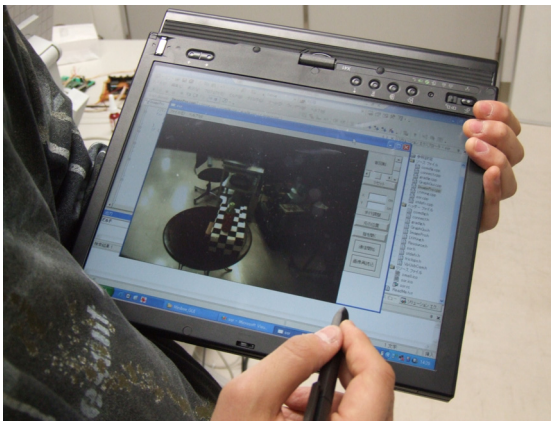

Fig. 9 GUI display

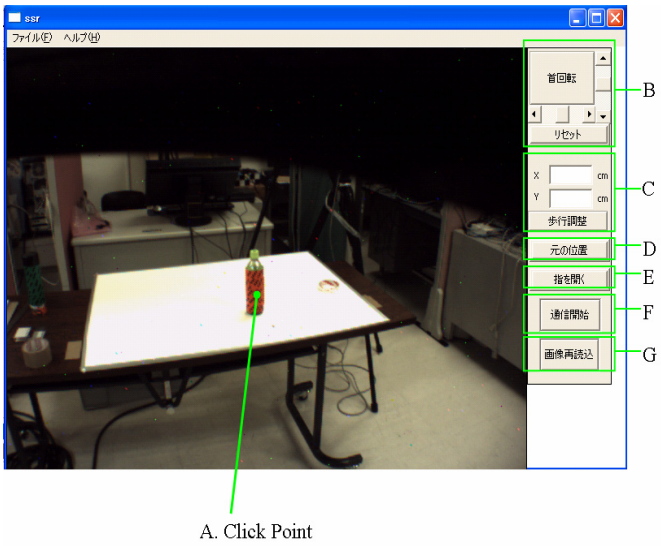

Fig. 10 Functions of GUI

C. Position adjusting button:

The standing position of humanoid robot can be adjusted manually by inputting the value of x direction and y direction and pushing the walking button.

D. Initial position button:

When this button is pushed after walking, HRP-2 moves to the initial standing position.

E. Open finger button:

When this button is pushed after grabbing the object, HRP-2 opens its finger.

F. Connect starting button:

After pushing this button, user can send commands to HRP-2 by socket connection.

G. Vision renew button

Pushing this button, the image of GUI on the display is renewed to the newest image Mini BEE has captured.

When a user clicks on the camera image and the calculated point is enough close to grasp the object for HRP-2, window A appears on the display. It is shown in Fig.11. The displayed numbers show the position for reaching the hand. Each of numbers (x, y, z) shows the depth (cm), the right (cm) and the height (cm) of the target point of the cylinder sequentially from the standing position of HRP-2. When "OK" button is pressed, HRP-2 starts to move the hand to the target point.

Otherwise, if HRP-2 stands on far from the target object, window B is appeared. The numbers of upper row show the position of clicked object and the lower shows the next standing position for grasping the target. The position is set front 0.6m, left 0.2m of the clicked object and we call it "Grasping position" . When "OK" button is pressed, HRP-2 starts to walk.

3.2 The Algorism of Grasping Action

・Judgment by Distance

When users click the object in the display, if the distance between HRP-2 and clicked object is over 1.0m, HRP-2 doesn't go to grabbing position at once for safety. In this

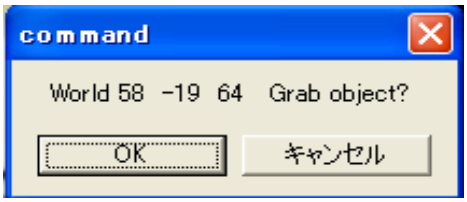

Fig. 11 Window A

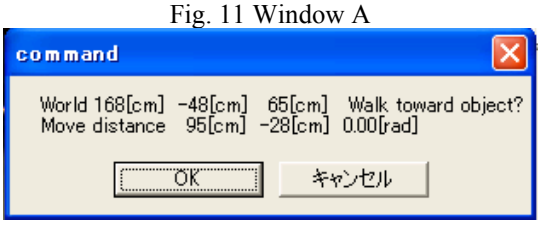

Fig. 12 Window B

case, HRP-2 walks to the position of (0.6+(d-1.0)/5) m in front and 0.2m in left side of the object. Here, d is the distance betweenHRP-2 and clicked point.

・Number of Detected Pixels

With the method mentioned in chapter 2.1, we set the threshold of detected pixels of cylinder 1200. If there are pixels more than this threshold, we can process conic fitting efficiently. When we clicked the object, if the detected pixels of cylinder are more than 1200, target point of cylinder is calculated. Otherwise, HRP-2 walks to the grabbing position.

・Judgment of the Calculation Success

If calculation of target point succeeds, it goes to the next judgment. Otherwise, calculation is tried again by clicking object.

・Judgment whether the Distance is Suitable for Grasping

In the values of standing position of HRP-2 from target point, if the value of depth (d) and value of left (l) satisfies the following condition, HRP-2 can start grabbing action.

$$0.55m < d < 0.65m \quad (12)$$

$$0.15m < l < 0.25m \quad (13)$$

Otherwise, HRP-2 walks to the grabbing position. The flowchart of the action algorithm control is shown in Fig. 13.

3.3 Result of Experiment

In this experiment, the position of cylinder was put 1736mm front, 403mm right and 786mm height from the initial standing location of HRP-2 (Fig.14). By executing this program, first, the distance between initial position of HRP-2 and cylinder is over 1.0m, so HRP-2 didn't go to the grabbing position at once. HRP-2 walked 1015mm front and 161mm right, thus it arrived at Second position. Then cylinder went out of sight, neck was turned to put it into the sight. Cylinder is clicked again. HRP-2 walked 136mm front and 48mm right and it arrived at the third position. Here is the grabbing position. Then HRP-2 turned neck again and the target point is calculated. Finally, HRP-2 started grabbing the cylinder.

The action process of grasping object is shown in Table 1 and Fig. 14. The scenery of action is shown in Fig. 15.

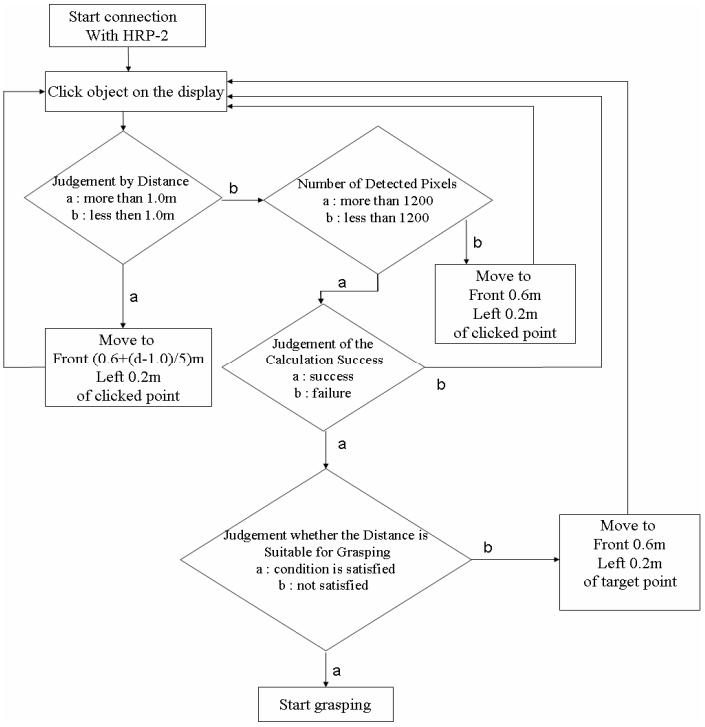

Fig. 13 Flow chart of control program

Table 1 Move process to grab object

	Initial position	Second position	Third position
Neck angle	Yaw:0, Pitch:0	Yaw: 0, Pitch:9	Yaw: 0,Pitch:19
Walk distance (mm)	x:1015, y: -161	X:136, y: -48	X: 0, y: 0
Grab position (mm)	x: 0, y: 0, z: 0	X: 0, y: 0, z: 0	x:586,y:-190,z:786

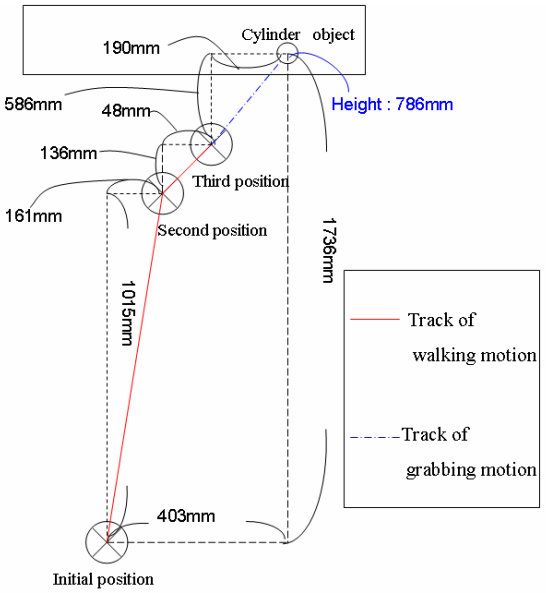

Fig. 14 Track to grab object

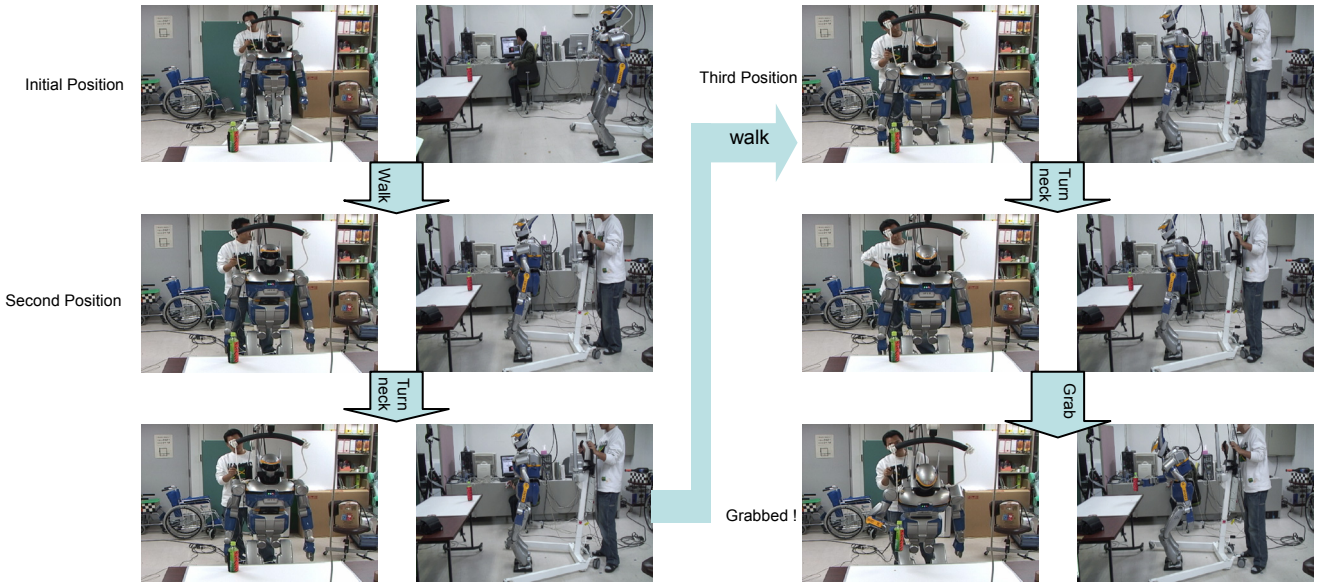

Fig. 15 Scenery of Experiment

4. CONCLUSIONS

In this research, the authors detected the center of gravity of the cylinder with a method combining oval estimation with conic fitting and color discrimination with L*a*b* color expression. The action command to HRP-2 is transmitted with the GUI and the grabbing experiment has been succeeded.

Future works require consideration of the action of humanoid robots after grabbing the object and creation of the grabbing action according to the shape of the cylinder. Furthermore, to adopt the humanoid robots for works and duties in construction site, the improvement of skillfulness, work speed and safety will be future problems.

5. ACKNOWLEDGEMENT

I would like to express my gratitude to Assistant Tomohiro Umetani in Nagoya City University who taught me courteously about the process of conic fitting and guided me how to push forward my research. Furthermore, this research was supported by MEXT under Grant-in-Aid for Creative Scientific Research (Project No. 13GS0018). I thank for the support heartily.

REFERENCES

[1] Junichiro MAEDA, Hiroo TAKADA, Yoshio ABE "Applicable possibility studies on a humanoid robot to cooperative work on construction site with a human worker" Proceedings of the 10th Symposium on Construction Robotics in Japan, pp49-56, 2004(Japanese).

[2] Kenji KANEKO, Fumio KANEHIRO, et al., "Humanoid Robot HRP-2" Proceedings of the 2004 IEEE International Conference on Robotics & Automation, pp. 1083-1090, 2004.

[3] Kensuke Harada, Shuuji Kajita, et al. "Real-Time Planning of Humanoid Robot's Gait for Force Controlled Manipulation" Proceedings of the 2004 IEEE International Conference on Robotics & Automation, pp 616-622, 2004.

[4] Naoto Kawauchi, Shigetoshi Shiotani, et al., "A Plant Maintenance Humanoid Robot System" Proceedings of the 2003 IEEE International Conference on Robotics & Automation, pp2973-2978, 2003.

[5] Kazuhiko Yokoyama, Hiroyuki Handa, et al. "Cooperative Works by a Human and a Humanoid Robot" Proceedings of the 2003 IEEE International Conference on Robotics & Automation, pp. 2985-2991, 2003.

[6] Hitoshi Hasunuma, Katsumi Nakashima, et al. , "A Tele-operated Humanoid Robot Drives a Backhoe" Proceedings of the 2003 IEEE International Conference on Robotics & Automation, pp. 2998-3004, 2003.

[7] Haruyoshi YAMAMOTO, Masato TSUKADA, Itaru KITAHARA, Yoshinari KAMEDA, and Yuichi OHTA "Color Calibration between Cameras for an Outdoor Mixed-Reality System" The Institute of Electronics, Information and Communication engineers, pp. 1-6, 2005,

[8] Y. Kanazawa and K. Kanatani, "Optimal conic fitting and reliability evaluation" IEICE Transactions on Information and Systems, Vol. E79-D, No. 9, pp. 1323-1328, 1996.

[9] K. kanatani, "Statistical Optimization for Geometric Computation" Theory and Practice, Elsevier Science, Amsterdam, 1996.